

An Experimental and Theoretical (DFT) Investigation of the Coordination Mode of 2,4-Dithiouracil (2,4-dtucH₂) in Copper(I) Complexes with 1,2-Bis(diphenylphosphanyl)benzene (dppbz): The Crystal Structures of [Cu(μ-Br)(dppbz)]₂ and [CuBr(dppbz)(2,4-dtucH₂)]

Paraskevas Aslanidis,^{*[a]} Philip J. Cox,^[b] Andreas Kaltzoglou,^[a] and Athanasios C. Tsipis^{*[c]}

Keywords: Copper / Density functional calculations / Phosphane ligands / S ligands

Novel copper(I) mixed-ligand complexes containing 1,2-bis(diphenylphosphanyl)benzene (dppbz) and 2,4-dithiouracil (2,4-dtucH₂) ligands have been synthesised by addition of the thione ligand to the dinuclear [Cu(μ-X)(dppbz)]₂ intermediate in acetonitrile/methanol or acetone solution. The molecular structures of both the precursor [Cu(μ-Br)(dppbz)]₂ and the [CuBr(dppbz)(2,4-dtucH₂)] complexes were established by single-crystal X-ray diffraction. Interestingly, the structure of the thione-free dimer involves two diphosphane-chelated Cu^I centres bridged by two bromide ligands, thus forming a non-planar Cu₂Br₂ core. The structure of [CuBr(dppbz)(2,4-dtucH₂)] corresponds to a four-coordinate Cu^I centre in a tetrahedral coordination environment with the heterocyclic dithione ligand being coordinated to the metal centre in a unidentate fashion through its exocyclic sulfur donor atom. The structural, bonding and electronic proper-

ties of the model complexes [Cu(μ-X)(dppbz)]₂ and [CuX(dppbz)(2,4-dtucH₂)] (X = Cl, Br, or I) are adequately described by DFT/B3LYP computational techniques. All model dinuclear [Cu(μ-X)(dppbz)]₂ complexes exhibit π-type MOs delocalised over the entire four-membered Cu(μ-X)₂Cu ring, thereby accounting for the near equivalency of the Cu–X bonds. Moreover, the [Cu(μ-X)(dppbz)]₂ dimers possess a σ-type MO corresponding to weak Cu...Cu bonding interactions, which further stabilize the Cu(μ-X)₂Cu ring. According to our calculations, the interaction energies of the 2,4-dtucH₂ ligand with the Cu^I centre are predicted to be about 13–16 kcal mol⁻¹. The coordination of the 2,4-dtucH₂ ligand is further stabilized by an X...H–N hydrogen bond that is perpendicular to the plane of the dppbz ligand.
(© Wiley-VCH Verlag GmbH & Co. KGaA, 69451 Weinheim, Germany, 2006)

Introduction

The coordination chemistry of heterocyclic thiones has grown enormously in the recent past, mainly because of their relevance to biological systems.^[1,2] The salient feature of these heterocyclic thioamides is their ability to bind to a metal centre in a variety of coordination modes. Along these lines a wealth of complexes exhibiting variable nuclearities and often unusual geometries have been synthesised and studied so far.^[1–7] A large number of mixed-ligand complexes of the univalent coinage metals, particularly those of Cu^I, incorporating tertiary arylphosphanes as a second, bulky soft donor ligand have been thoroughly investigated in an attempt to understand the factors that may affect the stoichiometric and geometrical preferences

of these compounds.^[3] In this context, some examples of three-coordinate Cu^I complexes, where the steric requirements of the phosphane ligands exert an influence on the coordination number, have also been reported.^[4] Moreover, a number of halo- or thione-S-bridged dinuclear mixed-ligand complexes have been synthesised and structurally well characterised.^[3,5] In contrast to the monodentate triarylphosphanes, didentate P-donor ligands, especially the oligomethylene-backboned symmetric diphosphanes formulated as Ph₂P(CH₂)_nPPh₂ (*n* = 1, 2 or 4), favour the formation of dinuclear complexes.^[6] On the other hand, the rigid *cis*-1,2-bis(diphenylphosphanyl)ethane (*cis*-dppen) and 1,3-bis(diphenylphosphanyl)propane (dppp) have been found to chelate at a single metal centre, yielding mononuclear pseudo-tetrahedral Cu^I species.^[7] Another didentate P-donor ligand capable of forming chelate five-membered symmetric rings is the sterically demanding 1,2-bis(diphenylphosphanyl)benzene, hereafter abbreviated as dppbz. Although dppbz has already been used extensively as a chelating ligand for many metal centres,^[8] no structurally characterised Cu^I or Ag^I derivatives of this rigid diphosphane, as far as we know, are currently known.

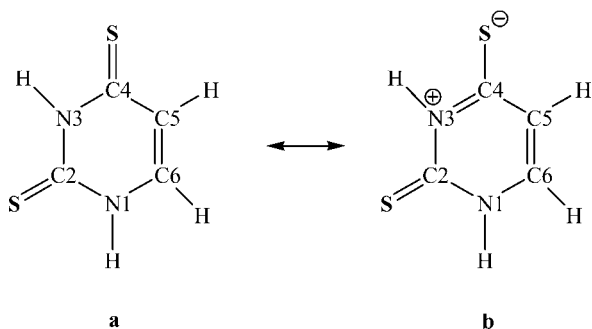
Among the heterocyclic thiones, the coordination properties of the thio derivatives of uracil, such as 2-thiouracil

[a] Aristotle University of Thessaloniki, Faculty of Chemistry, Inorganic Chemistry Laboratory, P. O. Box 135, 54124, Thessaloniki, Greece
E-mail: aslanidi@chem.auth.gr

[b] School of Pharmacy, The Robert Gordon University, Schoolhill, Aberdeen AB10 1FR, Scotland
E-mail: p.j.cox@rgu.ac.uk

[c] Section of Inorganic and Analytical Chemistry, Department of Chemistry, University of Ioannina, 45110 Ioannina, Greece
E-mail: attsipis@cc.uoi.gr

(2-tucH₂), 4-thiouracil (4-tucH₂) and 2,4-dithiouracil (2,4-dtucH₂) are of particular interest as these ligands have significant biological interest.^[9] Very recently, the gas-phase reactivity of uracil, 2-tucH₂, 4-tucH₂, and 2,4-dtucH₂ towards Cu⁺ and Cu²⁺ cations has been thoroughly investigated using electronic structure calculation methods.^[10] In this work we report on the synthesis, characterisation and electronic structure calculations of new copper(I) coordination compounds bearing dppbz and/or 2,4-dtucH₂ as ligands. In effect, what we want to address here is the coordination bonding mode of the versatile 2,4-dtucH₂ ligand (Scheme 1), which has two exocyclic sulfur donor atoms of different basicity that are capable of coordinating to Cu^I metal centres.



Scheme 1. Resonance structures of 2,4-dtucH₂.

Results and Discussion

Synthesis

The new compounds were prepared following a synthetic pathway that has already produced a number of mixed-ligand copper(I) halide complexes. Thus, 1 mmol of CuCl or CuBr was first treated with an equimolar quantity of dppbz to yield an intermediate adduct formulated as [CuX(dppbz)] (X = Cl, Br). This intermediate was then allowed to react with one equivalent of 2,4-dtucH₂ in refluxing dry acetonitrile for 2 h to afford the corresponding pure mixed-ligand complexes [CuX(dppbz)(2,4-dtucH₂)] (X = Cl: **1**; Br: **2**) in good yields. During the reaction of 2,4-dtucH₂ with CuBr, a small quantity of greenish yellow crystals was separated at the initial stages of the evaporation of the diluted acetonitrile mother liquid; their analytical and spectroscopic data were identical to those of the [CuBr(dppbz)] intermediate. In this way we were able to characterise the intermediate by X-ray crystallography as the thione-free dimer [CuBr(dppbz)]₂ (**3**). It should be noted that **3** is inert in the reactions with a number of heterocyclic thiones [e.g. 5-methyl-1,3,4-thiadiazole-2-thione (mtdztH) or 4-methyl-5-trifluoromethyl-4*H*-1,2,4-triazol-3(2*H*)-thione (mftztH)]. Treatment of CuI with equimolar quantities of dppbz readily yielded the intermediate 1:1 adduct [CuI(dppbz)]_x (**4**) as a white microcrystalline solid, which, however could not be converted into the corresponding [CuI(dppbz)(2,4-dtucH₂)] (**5**). Compound **5** was

obtained following a reverse synthetic procedure, i.e., by adding a twofold excess of the 2,4-dtucH₂ ligand to a Cu^I solution, followed by addition of dppbz. The orange-red precipitate formed before adding dppbz probably corresponds to the polymeric species [CuI(2,4-dtucH₂)]_x (**6**), which depolymerises upon addition of dppbz to give **5** as an orange solid. The analogous polymeric species [CuBr(2,4-dtucH₂)]_x (**7**) was also isolated as an orange-red powder following the same synthetic procedure. To investigate the ability of 2,4-dtucH₂ for further coordination to CuX through both exocyclic thione-S donor atoms, a series of reactions using variable stoichiometries and reaction conditions were carried out, but in all cases Cu^I complexes involving 2,4-dtucH₂ coordination in the mono-hapto or μ₂-coordination mode via the S donor atom at the 4-position were isolated.

All new complexes are diamagnetic, air-stable, microcrystalline solids that are moderately soluble in acetonitrile and only marginally soluble in chloroform and acetone. Their solutions in acetone and chloroform are non-conducting. The stoichiometry and structure of the complexes were confirmed by elemental analysis and spectroscopic measurements. Moreover, the molecular structures of [CuBr(dppbz)(dtucH₂)] (**2**) and [CuBr(dppbz)]₂ (**3**) were determined by X-ray crystallographic analyses.

Spectroscopy

The electronic absorption spectra of the new compounds in chloroform solution at room temperature show an intense, broad band with maxima in the region of 243–255 nm, which can be attributed, with reference to the absorption bands of the uncoordinated dppbz, to intraligand π*←π transitions on the phenyl groups of the phosphane ligand. Moreover, the spectra of compounds **1**, **2** and **5–7** display an additional broad band in the region of 285–310 nm, where the free thiones normally absorb. This band experiences a small red-shift as a consequence of the coordination to Cu^I and may be ascribed to a thione-originating intraligand transition. The IR spectra of compounds **1–3**, **6** and **7**, recorded in the range 4000–250 cm⁻¹, all show the expected strong phosphane bands, which remain practically unshifted upon coordination. Moreover, the spectra of compounds **1**, **2** and **4–7** contain all of the bands required by the presence of the heterocyclic thione ligand, with shifts due to coordination indicative of an exclusive S-coordination mode.

X-ray Structural Investigations

The X-ray crystal structures of [CuBr(dppbz)(dtucH₂)] (**2**) and [Cu(μ-Br)(dppbz)]₂ (**3**) corroborate the spectroscopic results discussed above. Selected bond distances and angles of complexes **2** and **3** are listed in Tables 1 and 2, respectively.

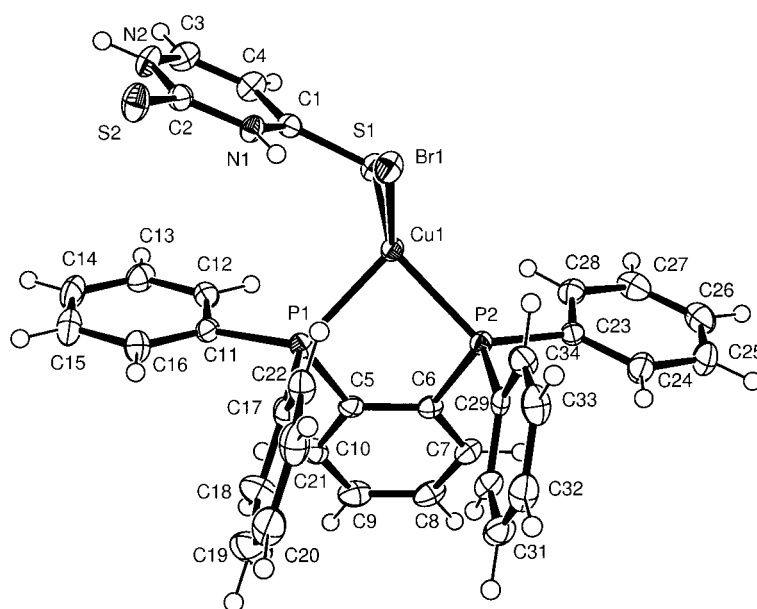
Table 1. Selected bond lengths [Å] and angles [°] for **2**.

Cu(1)–Br(1)	2.4366(3)	S(2)–C(2)	1.650(2)
Cu(1)–P(1)	2.2953(6)	P(1)–C(5)	1.838(2)
Cu(1)–P(2)	2.2393(6)	P(2)–C(6)	1.833(2)
Cu(1)–S(1)	2.2921(6)	C(5)–C(6)	1.408(3)
S(1)–C(1)	1.679(2)		
P(1)–Cu(1)–P(2)	86.73(2)	C(1)–S(1)–Cu(1)	105.24(7)
P(1)–Cu(1)–S(1)	108.37(2)	C(5)–P(1)–Cu(1)	99.68(7)
P(2)–Cu(1)–S(1)	120.10(2)	C(6)–P(2)–Cu(1)	101.34(7)
P(1)–Cu(1)–Br(1)	115.586(18)	P(1)–C(5)–C(6)	117.21(16)
P(2)–Cu(1)–Br(1)	118.836(18)	P(2)–C(6)–C(5)	118.10(16)
S(1)–Cu(1)–Br(1)	106.015(18)		
Hydrogen bonds			
N(1)–H(1)	0.8800	Br(1)···N(1)	3.3175(16)
NH(1)···Br(1)	2.5100	Br(1)···H(1)–N(1)	152°
N(2)–H(2)	0.8800	Br(1)···N(2)	3.1994(19)
NH(2)···Br(1)	2.4300	Br(1)···H(2)–N(2)	146°

Table 2. Selected bond lengths [Å] and angles [°] for **3**.

Cu(1)–Br(1)	2.4556(6)	Cu(1)–P(1)	2.2586(10)
Cu(2)–Br(1)	2.4958(6)	Cu(1)–P(2)	2.2549(11)
Cu(2)–Br(2)	2.4279(6)	Cu(2)–P(3)	2.2600(11)
Cu(1)–Br(2)	2.5317(6)	Cu(2)–P(4)	2.2546(11)
Cu(1)–Cu(2)	2.8410(6)		
Cu(1)–Br(1)–Cu(2)	70.022(17)	P(4)–Cu(2)–Br(2)	118.14(3)
Cu(2)–Br(2)–Cu(1)	69.859(17)	P(3)–Cu(2)–Br(1)	108.96(3)
P(1)–Cu(1)–P(2)	90.50(4)	P(3)–Cu(2)–Br(2)	121.41(4)
P(2)–Cu(1)–Br(1)	120.66(3)	P(4)–Cu(2)–Br(1)	110.55(3)
P(1)–Cu(1)–Br(1)	121.08(3)	Br(2)–Cu(2)–Br(1)	108.425(19)
P(2)–Cu(1)–Br(2)	107.09(3)	C(13)–P(1)–Cu(1)	102.10(12)
P(1)–Cu(1)–Br(2)	109.88(3)	C(14)–P(2)–Cu(1)	102.04(12)
Br(1)–Cu(1)–Br(2)	106.417(19)	C(43)–P(3)–Cu(2)	100.75(13)
P(4)–Cu(2)–P(3)	87.86(4)	C(44)–P(4)–Cu(2)	101.48(13)

Compound **2** crystallises in the monoclinic space group $P2_1/c$ with four formula units in the unit cell. Figure 1 depicts a perspective of the molecule showing the atom-labelling scheme.

Figure 1. Structure of complex **2** together with the atom-labelling scheme (50% probability ellipsoids with hydrogen atoms omitted for clarity).

The tetrahedral environment of the copper atom formed by the two P atoms of the chelating dppbz unit, one Br and one of the two exocyclic S donor atoms of the dithione ligand is considerably distorted, with the largest deviation from the ideal geometry being reflected by the P(1)–Cu(1)–P(2) and P(1)–Cu(1)–Br(1) angles of 86.61(2)° and 122.05(19)°, respectively, which are markedly different from the ideal tetrahedral value of 109.4°.

As expected, the carbon atoms of the phenylene backbone and the two adjacent phosphorus atoms are coplanar and the CuPCCP five-membered ring adopts an envelope conformation with the metal atom out of the plane containing the four diphos ligand donor atoms by 1.034(1) Å. The two phenyl rings on each phosphorus atom are nearly perpendicular to each other. However, the C(17)–C(22) and C(29)–C(34) phenyl rings have their planes in an almost parallel arrangement, with a π -stacking interaction of 3.827(1) Å between them. Likewise, the inclination of the pyrimidine ring to the C(11)–C(16) phenyl ring results in a π -stacking interaction of 4.116(1) Å. The two Cu–P distances [2.2393(6) and 2.2953(6) Å] are significantly different, but are within the limits of the range expected for tetrahedrally coordinated Cu^I.

The coordinated 2,4-dithiouracil ligand, which adopts its most stable dithione tautomeric form (**a**, Scheme 1) is coordinated to the Cu^I metal centre in a monodentate coordination mode through the S atom in the 4-position. Considering that the corresponding carbon–sulfur bond of the uncoordinated 2,4-dtuch₂ has been found to be significantly longer than that in the 2-position [1.684(6) vs. 1.645(6) Å],^[11] the favourable coordination of that specific sulfur atom can be interpreted as the inevitable consequence of its strong polarisation towards the amidic [–HN⁺=C(S[–])–] configuration (**b**). However, coordination to Cu^I does not affect these two bond lengths significantly.

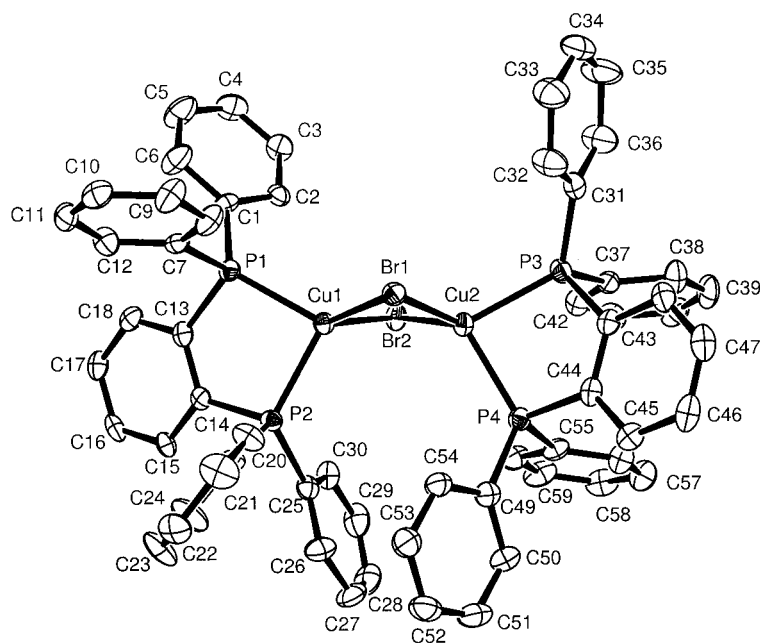


Figure 2. Structure of complex **3** together with the atom-labelling scheme (50% probability ellipsoids with hydrogen atoms omitted for clarity).

Likewise, the structural parameters within the heterocyclic backbone remain practically unaffected upon coordination.

Light-green single crystals of **3** were grown from the acetonitrile/methanol mother liquid of **2** during the earlier stages of the slow evaporation. Complex **3** crystallises in the monoclinic space group $P2_1$ with two formula units in the unit cell. The structure of **3**, together with the atom-labelling scheme, is shown in Figure 2.

The crystal structure features a dinuclear unit in which the two copper(I) centres are joined by two bromine bridges to form a four-membered Cu_2Br_2 core with a $\text{Cu}\cdots\text{Cu}$ separation distance of 2.8410(6) Å, which is suggestive of a weak metal–metal interaction, as further substantiated by the electronic structure calculations (vide infra). The strongly distorted tetrahedral coordination around each copper(I) central atom is completed by the two P donor atoms of the chelating dppbz unit.

The most salient, and quite unexpected, feature of the structure is the remarkable non-planarity within the Cu_2Br_2 central core. Unlike in other bromide-bridged dinuclear complexes that exhibit a strictly planar Cu_2Br_2 core, such as $[\text{Cu}(\mu_2\text{-Br})(\text{tmp})(\text{tzdtH})]_2$ (tmp = tri-*m*-tolylphosphane),^[5] the two main planes in **3** through Br(1), Cu(1), Br(2) and Br(1), Cu(2), Br(2) form a dihedral angle of 150.10(2)°, with Br(2) being displaced from the mean plane defined by Cu(1), Br(1) and Cu(2) by 0.7201(8) Å. The same uncommon non-planarity adopted by the Cu_2I_2 moiety previously observed in $[\text{Cu}(\mu_2\text{-I})(\text{dppet})]_2$ [dppet = *cis*-1,2-bis(diphosphanyl)ethane] is noteworthy.^[7b]

Each of the two CuPCCP five-membered chelate rings adopts the envelope conformation with the metal atoms out of the plane containing the four diphos ligand donor atoms by 0.665(3) and $-0.951(2)$ Å for Cu(1) and Cu(2), respectively. Consequently, the bite angles of the two diphosphane

units (Table 2) are clearly different, with the larger intraligand P–Cu–P angle belonging to the more distorted $\text{C}_2\text{P}_2\text{Cu}$ ring. The four individual Cu–P bonds lie in the narrow range of 2.2546(11)–2.2600(11) Å and match those observed in $[\text{Cu}(\text{dppet})_2]\text{PF}_6$,^[12] as well as in other copper(I)–diphosphane complexes having a tetrahedral coordination environment.^[6,7] Moreover, there are four clearly different Cu–Br bond lengths within the Cu_2Br_2 backbone, lying in the range 2.4279(6)–2.5316(6) Å.

Computational Studies Using DFT

In an attempt to understand some marked structural features of the complexes under investigation, we performed electronic structure calculations based on density functional theory for compounds **2** and **3**, as well as for some related model species. To obtain a computationally convenient size for the compounds, we used models resulting from substitution of the phenyl groups of the diphosphane ligands by H atoms. The use of such models does not alter the description of the “core” region of the compounds and is ultimately the most efficient and productive route to modelling the electronic structure and related properties of relatively big-sized copper(I) complexes. In particular, we sought an explanation for the exclusive coordination of 2,4-dithiouracil through the thione-S atom at C(4) and explored the origin of the unexpected bend of the Cu_2Br_2 central core in compound **3**.

Equilibrium Geometries, Electronic Structure and Bonding Mechanism in the Series of Model Mononuclear Complexes $[\text{CuX}(\text{dphz})]$ [$X = \text{Cl}, \text{Br}, \text{or I}$; $\text{dphz} = 1,2\text{-bis}(\text{diphosphanyl})\text{benzene}$]

Selected structural and electronic properties of the mononuclear complexes $[\text{CuX}(\text{dphz})]$ ($X = \text{Cl}, \text{M1}$; $\text{Br}, \text{M2}$; $\text{I},$

M3) computed at the B3LYP/DGDZVP level of theory are given in Table 3.

All [CuX(dpbz)] species are three-coordinate Cu^I complexes that adopt a trigonal planar structure with the central copper(I) atom and the three donor atoms lying in a plane. As is to be expected, the Cu–X bond lengths increase upon going from the chloro to bromo to iodo derivative, which is compatible with the computed $\nu(\text{Cu–X})$ stretching vibrational frequencies at 354, 260 and 235 cm⁻¹, respectively. However, no other significant structural differences could be observed for the [CuX(dpbz)] (X = Cl, Br or I) complexes. Based on the HOMO–LUMO energy gap – the hardness values (η) are shown in Table 3 – one would expect the tendency for dimerisation to follow the order **M3** > **M2** > **M1**.

The most relevant molecular orbitals of the mononuclear complexes [CuX(dpbz)] related to the bonding mechanism are depicted schematically in Scheme 2. According to the natural bond orbital (NBO) population analysis, the Cu^I centre acquires a positive natural atomic charge of about 0.61–0.7|e|. Moreover, the natural electron configuration (*nec*) indicates that the electron density is mainly transferred to the 4s orbital of the copper(I) atom. The nature of the

halide ligand does not affect the natural electron configuration of the central Cu^I atom significantly. Interestingly, the computed bond overlap populations (*bop*) of the Cu–Br, Cu–Cl and Cu–I bonds are of almost equal size.

It can be seen that the Cu–X bond is a composite bond that acquires a partial double-bond character involving both σ and π components. The HOMO corresponds to a π^* -antibonding Cu–X interaction that is strongly polarized towards the halide ligand X. Below the HOMO there is a set of σ - (HOMO–2) and π -bonding MOs (HOMO–3 and HOMO–6) that correspond to Cu–X interactions as well as describing the σ and π dative bonding of the halide ligands. Finally, the LUMO is delocalised over the benzene ring of the diphosphane ligand.

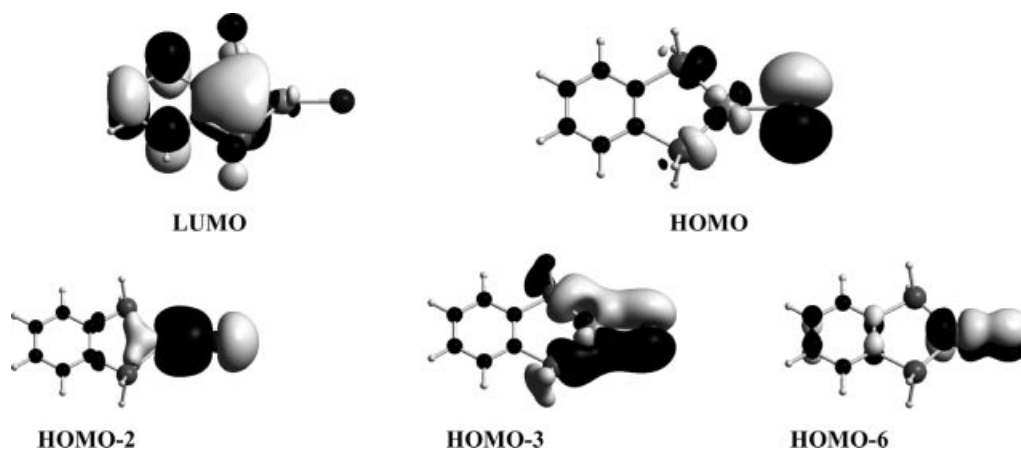
Equilibrium Geometries, Electronic Structure and Bonding Mechanism of the Dinuclear Compounds [Cu(μ -X)-(dpbz)]₂ (X = Cl, Br or I)

Selected structural parameters and electronic properties of the dinuclear compounds [Cu(μ -Cl)(dpbz)]₂ (**M4**), [Cu(μ -Br)(dpbz)]₂ (**M5**) and [Cu(μ -I)(dpbz)]₂ (**M6**) computed at the B3LYP/DGDZVP level of theory are compiled in Table 4.

Table 3. Selected structural parameters and electronic properties of the mononuclear complexes [CuX(dpbz)] (X = Br or Cl) computed at the B3LYP/DGDZVP level.

Property	[CuCl(dpbz)] (M1)	[CuBr(dpbz)] (M2)	[CuI(dpbz)] (M3)
$R_c(\text{Cu–X})$ [Å]	2.175	2.307	2.500
$R_c(\text{Cu–P}_1)$ [Å]	2.314	2.316	2.317
$\theta_c(\text{P–Cu–X})$ [°]	135.9	135.8	135.8
$\theta_c(\text{P–Cu–P})$ [°]	88.6	88.6	88.6
μ_c [D]	11.09	11.34	11.75
η [eV] ^[a]	1.78	1.70	1.59
q_{Cu} ^[b]	0.70	0.67	0.61
q_{X}	–0.78	–0.75	–0.70
q_{P}	0.23	0.23	0.23
<i>bop</i> (Cu–X) ^[c]	0.25	0.26	0.28
<i>bop</i> (Cu–P)	0.21	0.21	0.21
<i>nec</i> (Cu) ^[d]	4s ^{0.41} 3d ^{9.84}	4s ^{0.43} 3d ^{9.86}	4s ^{0.46} 3d ^{9.87}
<i>nec</i> (X)	3s ^{1.96} 3p ^{5.80}	4s ^{1.96} 4p ^{5.78}	5s ^{1.95} 5p ^{5.74}
<i>nec</i> (P)	3s ^{1.45} 3p ^{3.24}	3s ^{1.45} 3p ^{3.24}	3s ^{1.45} 3p ^{3.24}

[a] Hardness $\eta = (\epsilon_{\text{LUMO}} - \epsilon_{\text{HOMO}})/2$. [b] Natural charges. [c] Mulliken bond-overlap population. [d] Natural electron configuration.



Scheme 2. The most relevant molecular orbitals of the mononuclear complex [CuBr(dpbz)] (isodensity contours of 0.03 a.u.). The relevant MOs for [CuCl(dpbz)] and [CuI(dpbz)] are analogous.

Table 4. Selected structural parameters and electronic properties of the dinuclear model compounds [Cu(μ-X)(dpbz)]₂ (X = Cl, Br or I) computed at the B3LYP/DGDZVP level.

Property	[Cu(μ-Cl)(dpbz)] ₂ (M4)	[Cu(μ-Br)(dpbz)] ₂ (M5)	[Cu(μ-I)(dpbz)] ₂ (M6)
$R_e(\text{Cu-X})$ [Å]	2.402	2.525	2.720
$R_e(\text{Cu-P}_1)$ [Å]	2.316	2.327	2.335
$R_e(\text{Cu}\cdots\text{Cu})$ [Å]	2.972	2.948	2.887
$\theta_e(\text{P-Cu-X})$ [°]	116.2	114.7	112.4
$\theta_e(\text{P-Cu-P})$ [°]	89.1	88.8	88.5
$\theta_e(\text{Cu-X-Cu})$ [°]	76.4	71.5	64.1
$\theta_e(\text{X-Cu-X})$ [°]	103.6	108.5	115.9
μ_e [D]	0.00	0.00	0.00
η [eV] ^[a]	2.02	2.00	2.40
q_{Cu} ^[b]	0.75	0.70	0.62
q_{X}	-0.78	-0.75	-0.67
q_{P}	0.24	0.24	0.24
$bop(\text{Cu-X})$ ^[c]	0.13	0.15	0.16
$bop(\text{Cu-P})$	0.12	0.13	0.12
$nec(\text{Cu})$ ^[d]	4s ^{0.34} 3d ^{9.86}	4s ^{0.39} 3d ^{9.87}	4s ^{0.42} 3d ^{9.90}
$nec(\text{X})$	3s ^{1.95} 3p ^{5.82}	4s ^{1.95} 4p ^{5.78}	5s ^{1.94} 5p ^{5.72}
$nec(\text{P})$	3s ^{1.46} 3p ^{3.22}	3s ^{1.46} 3p ^{3.22}	3s ^{1.46} 3p ^{3.22}

[a] Hardness $\eta = (\epsilon_{\text{LUMO}} - \epsilon_{\text{HOMO}})/2$. [b] Natural charges. [c] Mulliken bond-overlap population. [d] Natural electron configuration.

As is to be expected, the dicopper(I) compounds adopt a “diamond like” structure of C_{2h} symmetry with the plane of the Cu(μ-X)₂Cu “rhombus” bisecting the P–Cu–P bond angles and being perpendicular to the plane of the diphosphane ligands. The four equivalent Cu–X bonds defining the Cu(μ-X)₂Cu “rhombus” are elongated by about 0.2 Å compared to the corresponding Cu–X bonds of the monomers. The calculated structural parameters are in line with those of the “real” complex **3** derived from the X-ray structural analysis. However, the non-planarity of the Cu₂Br₂ central core of complex **3** is not observed for the Cu₂X₂ core in the optimised structures of the model compounds **M4**, **M5**, and **M6**, thus indicating that steric and/or crystal-packing effects in the solid state should be responsible for the Cu₂Br₂ folding across the Br⋯Br line and the non-equivalent coordination spheres around the two Cu^I metal centres.

To verify this hypothesis, the rigid and relaxed PES of the “real” complex **3** and the model compound **M5** were calculated at the B3LYP/DGDZVP level of theory. It was found that the bending of the Cu₂Br₂ core in the “real” complex **3** and the model compound **M5** demands only 0.6 and 0.4 kcal mol⁻¹, respectively, thus indicating a very flat potential energy surface for both complexes. Therefore, factors such as the 4.298-Å π-stacking interaction between two almost parallel phenyl groups of the dpbz ligand could enforce the bending of the Cu₂Br₂ core in the real complex **3**. It should be noted that in an analogous dinuclear Ag^I complex containing bulky diphosphane or diarsane ligands the folding of the Ag(μ-Br)₂Ag core has been attributed to steric strain in the crystal.^[13] The intermetallic Cu⋯Cu distance follows the order **M4** > **M5** > **M6**, in line with our previous results^[7a] on analogous systems with general formula [Cu(μ-X)(PH₃)₂]₂ (X = Cl, Br or I), as well to the observations made by Soloveichic et al.^[14] in the framework of EHMO theory for the complexes [L_nCu(μ-X)CuL_n] ($n = 1$ or 2 , L = PR₃). Alvarez et al.^[15] have also found from MP2 and B3LYP calculations that the Cu⋯Cu distance in

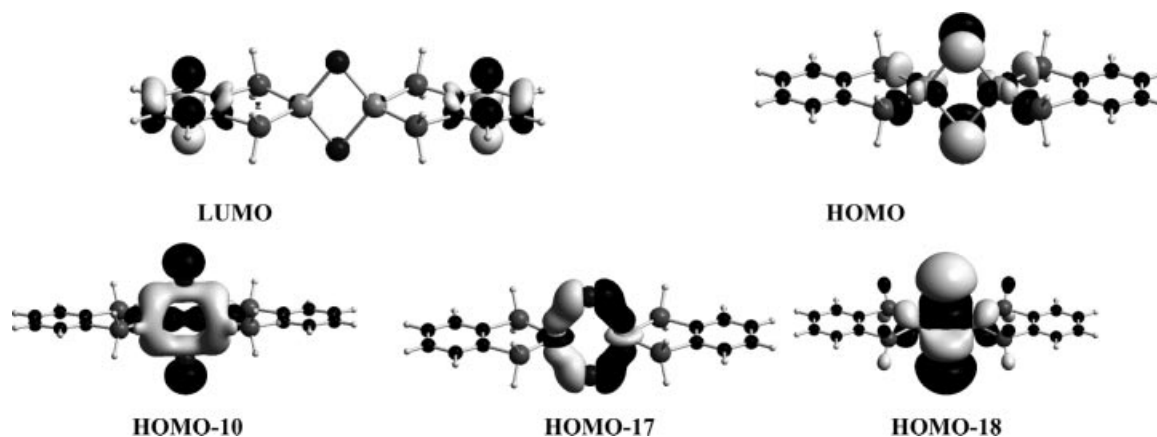
a series of [CuXL]₂ (X = Cl, Br or I) complexes decreases upon increasing the size of the bridging halide ligand. The X–Cu–X bond angle in **M6** was found to be more obtuse relative to that found for **M5** or **M4**, while the opposite holds true for the Cu–X–Cu bond angle (Table 4).

The computed $\nu_{\text{sym}}(\text{X-Cu-X})$ stretching vibrational frequencies at 140, 110 and 87 cm⁻¹ for the chloro, bromo and iodo derivatives, respectively, are compatible with the elongated Cu–X bonds in the dimers. The same also holds true for the computed $\nu_{\text{sym}}(\text{Cu-X-Cu})$ stretching vibrational frequencies at 202, 172 and 160 cm⁻¹ for **M4**, **M5** and **M6**, respectively.

All [Cu(μ-X)(dpbz)]₂ (X = Cl, Br, or I) molecules are predicted to be thermodynamically more stable than the corresponding monomers; the calculated heat of reaction $\Delta_{\text{R}}H$ for the dimerisation process was found to be 25–26 kcal mol⁻¹ at the B3LYP/DGDZVP level of theory. In addition, both **M4** and **M5** exhibit almost equal HOMO–LUMO energy gaps as well as hardness values, indicating comparable stability. On the other hand, **M6** exhibits the highest HOMO–LUMO energy gap and hardness value, and is expected to be the most stable amongst the [Cu(μ-X)(dpbz)]₂ (X = Cl, Br, or I) complexes.

No significant differences could be observed between the natural and net atomic charges on the Cu^I bridging halide and phosphorus donor atoms of **M4**, **M5** and **M6** (Table 4). The Cu^I metal centres acquire positive natural charges of about 0.6–0.8 |e|, while the halide bridging ligands acquire negative natural charges of around -0.7 |e|. According to the natural electron configurations, the electron density is mainly transferred from the valence p atomic orbitals of the bridging halide ligands to the 4s orbitals of the Cu^I metal centres.

The most important MOs of the [Cu(μ-X)(dpbz)]₂ dimers are depicted in Scheme 3. The HOMO corresponding to π* antibonding Cu–X interactions is polarized towards the bridging halide ligands, while the LUMO is delocalised over the benzene rings of the diphosphane ligands. There



Scheme 3. The most important molecular orbitals of the dinuclear complex $[\text{Cu}(\mu\text{-Br})(\text{dppbz})]_2$ (isodensity contours of 0.03 a.u.). The relevant MOs for $[\text{Cu}(\mu\text{-Cl})(\text{dppbz})]_2$ and $[\text{Cu}(\mu\text{-I})(\text{dppbz})]_2$ are analogous.

are σ -type MOs (HOMO–17 and HOMO–18) delocalised over the entire four-membered $\text{Cu}(\mu\text{-X})_2\text{Cu}$ ring. The delocalisation of the σ -electron density over the $\text{Cu}(\mu\text{-X})_2\text{Cu}$ rhombus having eight framework electrons^[16] could probably account for the almost equivalent Cu–X bonds. Interestingly, all $[\text{Cu}(\mu\text{-X})(\text{dppbz})]_2$ dimers exhibit a σ -type MO (HOMO–10), which suggests the existence of weak intermetallic $\text{Cu}\cdots\text{Cu}$ interactions.

Equilibrium Geometries, Electronic Structure and Bonding Mechanism of Mononuclear $[\text{CuX}(\text{dppbz})(2,4\text{-dtucH}_2)]$ ($X = \text{Cl}, \text{Br}$ or I) Complexes

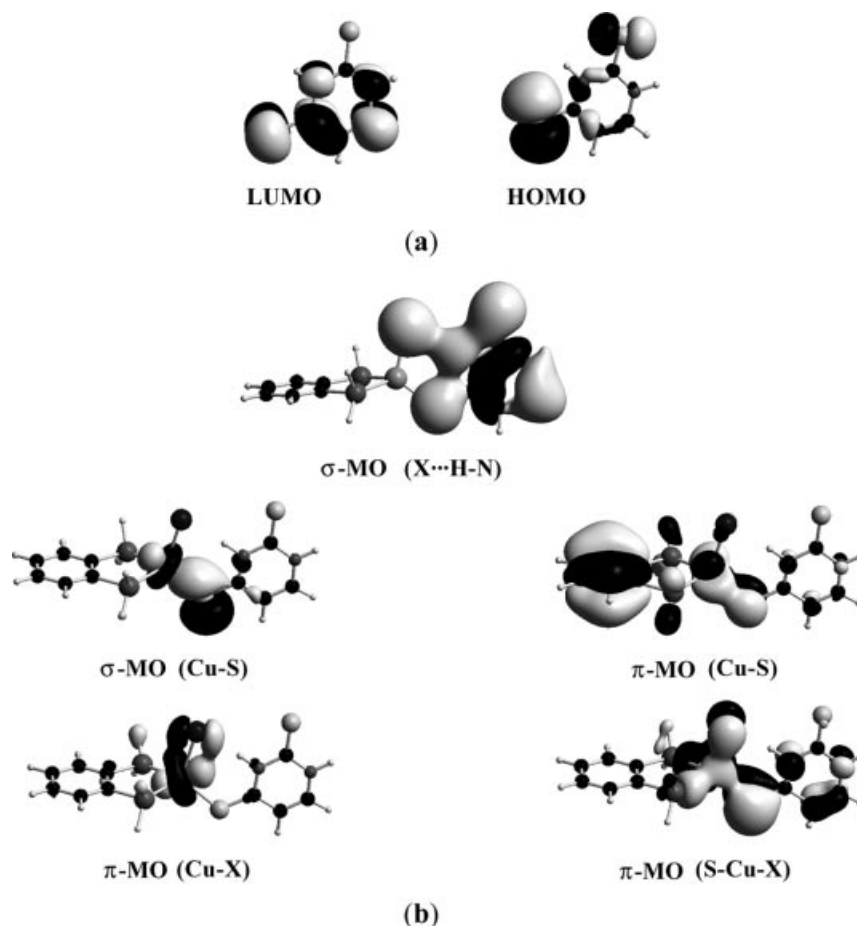
Selected structural parameters and electronic properties of the model compounds mononuclear $[\text{CuCl}(\text{dppbz})(2,4\text{-dtucH}_2)]$ (**M7**), $[\text{CuBr}(\text{dppbz})(2,4\text{-dtucH}_2)]$ (**M8**) and $[\text{CuI}(\text{dppbz})(2,4\text{-dtucH}_2)]$ (**M9**) computed at the B3LYP/DGDZVP level of theory are summarised in Table 5.

The complexes are four-coordinate with a tetrahedral coordination environment. The calculated structural parameters of **M8** are in excellent agreement with those obtained from the X-ray structural analysis of the “real” complex **2**. The most remarkable structural difference between **M8** and **2** is the orientation of the 2,4-dithiouracil ring – in **M7**, **M8** and **M9** the plane of the 2,4-dithiouracil ring is perpendicular to the plane of the diphosphane ligand and bisects the P–Cu–P bond angle. The 2,4-dithiouracil ligand in **M7**, **M8** and **M9** is further stabilized by a hydrogen bond between the halide ligand and an H atom of the 2,4-dithiouracil. The calculated $\text{X}\cdots\text{H}$ distances are predicted to be 2.113, 2.302 and 2.597 Å for **M7**, **M8** and **M9**, respectively. The H-bond formation is reflected in the computed $\text{X}\cdots\text{H}$ *bop* values, which were found to be 0.16, 0.14 and 0.12 for **M7**, **M8** and **M9**, respectively, as well as in the existence of a MO, with a σ component (Scheme 4, **b**), describing the

Table 5. Selected structural parameters and electronic properties of the mononuclear model compounds $[\text{CuX}(\text{dppbz})(2,4\text{-dtucH}_2)]$ ($X = \text{Cl}, \text{Br}$ or I) computed at the B3LYP/DGDZVP level.

Property	$[\text{CuCl}(\text{dppbz})(2,4\text{-dtucH}_2)]$ (M7)	$[\text{CuBr}(\text{dppbz})(2,4\text{-dtucH}_2)]$ (M8)	$[\text{CuI}(\text{dppbz})(2,4\text{-dtucH}_2)]$ (M9)
$R_e(\text{Cu-X})$ [Å]	2.324	2.451	2.647
$R_e(\text{Cu-P}_1)$ [Å]	2.341	2.348	2.356
$R_e(\text{Cu-S})$ [Å]	2.336	2.346	2.349
$\theta_e(\text{P-Cu-X})$ [°]	105.2	105.4	105.7
$\theta_e(\text{P-Cu-P})$ [°]	88.0	87.8	87.4
$\theta_e(\text{P-Cu-S})$ [°]	120.0	118.8	116.3
$\theta_e(\text{S-Cu-X})$ [°]	114.6	116.7	120.3
μ_e [D]	6.62	7.14	8.11
η [eV] ^[a]	3.31	3.12	2.77
q_{Cu} ^[b]	0.71	0.69	0.65
q_X	-0.77	-0.75	-0.71
q_P	0.23	0.24	0.23
q_S	-0.21	-0.20	-0.20
<i>bop</i> (Cu–X) ^[c]	0.17	0.19	0.21
<i>bop</i> (Cu–P)	0.15	0.15	0.15
<i>bop</i> (Cu–S)	0.20	0.21	0.20
<i>nec</i> (Cu) ^[d]	$4s^{0.37}3d^{9.86}$	$4s^{0.39}3d^{9.87}$	$4s^{0.41}3d^{9.88}$
<i>nec</i> (X)	$3s^{1.96}3p^{5.80}$	$4s^{1.96}4p^{5.78}$	$5s^{1.96}5p^{5.75}$
<i>nec</i> (P)	$3s^{1.46}3p^{3.23}$	$3s^{1.46}3p^{3.22}$	$3s^{1.46}3p^{3.23}$
<i>nec</i> (S)	$3s^{1.73}3p^{4.44}$	$3s^{1.73}3p^{4.44}$	$3s^{1.73}3p^{4.43}$

[a] Hardness $\eta = (\epsilon_{\text{LUMO}} - \epsilon_{\text{HOMO}})/2$. [b] Natural charges. [c] Mulliken bond-overlap population. [d] Natural electron configuration.



Scheme 4. The most important molecular orbitals of 2,4-dithiouracil (a) and the mononuclear compound [CuBr(dp bz)(2,4-dtucH₂)] (b) (isodensity contours of 0.03 a.u.). the relevant MOs for [CuCl(dp bz)(2,4-dtucH₂)] and [CuI(dp bz)(2,4-dtucH₂)] are analogous.

X \cdots H interaction. The latter introduces an elongation to the N–H bond only about 0.03–0.02 Å in the 2,4-dithiouracil ligand with respect to that of the “free” ligand.

The computed unscaled $\nu(\text{N–H})$ stretching vibrational frequencies appear at 3002, 3068 and 3160 cm^{-1} for **M7**, **M8** and **M9**, respectively, while in the “free” 2,4-dithiouracil ligand it appears at 3564 cm^{-1} . The strong shift of the $\nu(\text{N–H})$ stretching vibrational band towards lower frequencies upon coordination of the 2,4-dithiouracil ligand to the Cu^I centre is indicative of the involvement of the H atom in H-bond formation with the halide ligand. In all [CuX(dp bz)(2,4-dtucH₂)] (X = Cl, Br, or I) complexes the X \cdots H–N moiety is almost linear, the calculated X \cdots H–N bond angle being equal to 175–177°. On the other hand, the S–Cu–X and Cu–S–C bond angles were found to be smaller, ranging from 114–120° and 110–114°, respectively. Coordination of 2,4-dithiouracil to the Cu^I centre does not alter its structure significantly. However, in the [CuX(dp bz)(2,4-dtucH₂)] (X = Cl, Br, or I) complexes the coordination of the 2,4-dithiouracil through the S donor atom in the 4-position lengthens the C=S bond by about 0.03 Å. This could be attributed to electron-density transfer from the C=S group of the 2,4-dithiouracil ligand to the Cu^I centre, leading to formation of the Cu–S coordination bond. The latter has a composite nature and exhibits both

σ and π components, as can be seen from the corresponding MOs shown in Scheme 4b. The electron density is transferred from the HOMO of the 2,4-dithiouracil ligand, which is a non-bonding (lone pair) p-type MO localised mainly on the S donor atom at the 4-position and to a lesser extent on the S atom at the 2-position (Scheme 4a), to a vacant orbital of the Cu^I metal centre, thus forming the $\sigma(\text{Cu}\leftarrow\text{S})$ dative coordination bond. Obviously, the nature of the HOMO accounts well for the inability of the S atom at the 2-position to act as a second donor atom coordinated to another Cu^I metal centre. In addition, there is π back-bonding through the interaction of an occupied orbital of the Cu^I centre with the LUMO of the 2,4-dithiouracil ligand, which is a delocalised π^* -type MO having a high contribution from the 3p orbitals of the S(4) acceptor atom (Scheme 4a). The Cu–S coordination bond is relatively weak, with a predicted bond-dissociation energy (BDE) of 16.2, 14.8 and 13.2 kcal mol^{-1} for **M7**, **M8** and **M9**, respectively, at the B3LYP/DGDZVP level.

Upon coordination of the 2,4-dithiouracil ligand to the [CuX(dp bz)] (X = Cl, Br, or I) fragment the Cu–X bond is elongated by about 0.14–0.15 Å. This elongation is accompanied by a decrease of the *bop* values compared to those found for the [CuX(dp bz)] fragments. The coordination of the 2,4-dithiouracil to the Cu^I centre of the

[CuX(dpbz)] fragments does not affect the natural atomic charges significantly, while the same holds true for the natural electron configurations of the respective atoms.

Conclusions

We have described the synthesis and structural characterisation of copper(I) coordination compounds bearing 1,2-bis(diphenylphosphanyl)benzene (dppbz) and/or 2,4-dithiouracil (2,4-dtucH₂) as ligands. The reaction of 1,2-bis(diphenylphosphanyl)benzene (dppbz) with copper(I) halides yields [CuX(dppbz)] adducts, which for X = Br corresponds to a dimer of the formula [Cu(μ-Br)(dppbz)]₂ containing a non-symmetrical, bent Cu₂Br₂ core structure. The Cu...Cu separation distance of 2.8410(6) Å is indicative of weak intermetallic interactions. The latter is further corroborated by DFT calculations on the model dinuclear compound [Cu(μ-Br)(dpbz)]₂, which exhibits a characteristic σ-type MO (HOMO-10) describing these weak intermetallic Cu...Cu interactions. However, the non-planarity of the central Cu₂Br₂ core is not observed for the Cu₂X₂ core in the optimised model structures, thus indicating that π-stacking interactions between the two almost parallel phenyl groups of the diphosphane ligand are probably responsible for the Cu₂Br₂ folding across the Br...Br axis. The presence of σ-type MOs delocalised over the entire four-membered Cu(μ-X)₂Cu ring containing eight framework electrons accounts for the equivalent Cu–X bonds of the rhombus. The dimerisation energy of the [Cu(μ-X)(dpbz)]₂ (X = Cl, Br, or I) dimers is predicted to be 25–26 kcal mol⁻¹ at the B3LYP/DGDZVP level. The [CuBr(dppbz)]₂ dimer and its chloride and iodide analogues prove to be good precursors for the preparation of other derivatives and are used, in the course of the present study, for the synthesis of heteroleptic complexes which contain, besides the chelating dppbz, a 2,4-dithiouracil ligand. In line with theoretical predictions, the 2,4-dithiouracil ligand, which adopts the dithione form as its stable conformation, acts as a monodentate ligand that is coordinated to the metal ion exclusively through its thione-S atom at the 4-position. The nature of the HOMO – a non-bonding, lone-pair, π-type MO localised mainly on the S donor atom at the 4-position – accounts well for the inability of the S atom at the 2-position to act as a second donor to another Cu^I centre. Moreover, the 2,4-dithiouracil ligand in the [CuX(dpbz)(dtucH₂)] complexes is predicted to be loosely associated with the Cu^I centre, the interaction energies being 13–16 kcal mol⁻¹ at the B3LYP/DGDZVP level.

Experimental Section

Materials and Instrumentation: Commercially available copper(I) chloride, bromide and iodide, and 1,2-bis(diphenylphosphanyl)benzene were used as received, while pyrimidine-2,4-dithione (Aldrich) was recrystallised from hot ethanol prior to use. All the solvents were purified by standard methods and stored over molecular sieves. IR spectra in the region of 4000–200 cm⁻¹ were obtained in

KBr discs with a Perkin–Elmer 1430 spectrophotometer, while a Perkin–Elmer–Hitachi 200 spectrophotometer was used to obtain the electronic absorption spectra. Melting points were measured in open tubes with a STUART scientific instrument and are uncorrected. Molar conductivities, magnetic susceptibility measurements and elemental analyses for carbon, nitrogen and hydrogen were performed as described elsewhere.^[17]

Computational Details: The structural, electronic and energetic properties of all compounds were computed with Becke's three-parameter hybrid functional^[18] combined with the Lee–Yang–Parr correlation functional,^[19] abbreviated as B3LYP, using the DGDZVP basis set.^[20] We used the all-electron, double-zeta valence DGDZVP basis set, which is comparable with the 6-31G(d) level,^[21] because it has been found previously^[22] that it provides a satisfactory description of the structural and energetic properties of analogous Cu^I complexes (overall closer to the experiment) but it is less time consuming for computations with such big-sized transition metal complexes than the larger 6-31G(d,p) basis set. No constraints were imposed on the geometry in any of the calculations. Full geometry optimisation was performed for each structure using Schlegel's analytical gradient method^[23] and the attainment of the energy minimum was verified by calculating the vibrational frequencies that result in an absence of imaginary eigenvalues. All calculations were performed using the Gaussian 03 suite of programs.^[24]

Crystal Structure Determination: Single crystals suitable for crystal structure analysis were obtained by slow evaporation of acetonitrile/methanol solutions of the complexes at room temperature. X-ray diffraction data were collected on an Enraf–Nonius Kappa CCD area-detector diffractometer. The programs DENZO^[25] and COLLECT^[26] were used for data collection and cell refinement, respectively. Details of crystal and structure refinement are shown in Table 6. The structures were solved using the program SIR97^[27] and refined with SHELX-97.^[28] Molecular plots were obtained with the program ORTEP-3.^[29]

CCDC-243707 (for **2**) and -269670 (for **3**) contain the supplementary crystallographic data for this paper. These data can be obtained free of charge from The Cambridge Crystallographic Data Centre via www.ccdc.cam.ac.uk/data_request/cif.

Synthesis of Complexes 1 and 2: 1,2-Bis(diphenylphosphanyl)benzene (223.2 mg, 0.1 mmol) was added to a suspension of CuCl or CuBr (0.5 mmol) in 30 mL of dry acetonitrile and the mixture was stirred for 2 h at 50 °C, during which time a greenish precipitate was formed. A solution of pyrimidine-2,4-dithione (0.5 mmol) in a small amount (≈20 mL) of methanol was then added and the reaction mixture was stirred under reflux for two hours, whereupon the precipitate gradually disappeared. The resulting clear solution was filtered off and left to evaporate at ambient temperature. The microcrystalline solid, which was deposited upon standing for several days, was filtered off and dried in vacuo.

[CuCl(dppbz)(2,4-dtucH₂)] (1): Orange-red solid (125 mg, 70%), m.p. 261 °C. C₃₄H₂₈ClCuN₂P₂S₂ (689.70): calcd. C 59.21, H 4.09, N 4.06; found C 59.75, H 4.05, N 3.93. IR: $\tilde{\nu}$ = 3446 m, 3050 m, 1599 s, 1570 vs, 1532 vs, 1480 m, 1435 m, 1342 s, 1215 s, 1198 s, 1100 s, 859 m, 741 s, 692 s, 520 s, 493 s, 467 m cm⁻¹. UV/Vis (CHCl₃): λ_{max} (log ϵ) = 262 nm (3.68), 298 (3.69), 392 (3.31).

[CuBr(dppbz)(2,4-dtucH₂)] (2): Orange-red crystals (130 mg, 70%), m.p. 265 °C. C₃₄H₂₈BrCuN₂P₂S₂ (734.15): calcd. C 55.63, H 3.84, N 3.82; found C 55.91, H 3.88, N 3.79. IR: $\tilde{\nu}$ = 3457 m, 3147 w, 3070 m, 1618 m, 1599 vs, 1531 vs, 1479 s, 1435 s, 1341 m, 1215 s, 1196 vs, 1099 vs, 1068 m, 768 s, 740 s, 692 vs, 519 vs, 492 s, 441 s cm⁻¹.

Table 6. Crystal data and structure refinements for **2** and **3**.

	2	3
Molecular formula	C ₃₄ H ₂₈ BrCuN ₂ P ₂ S ₂	C ₆₀ H ₄₈ Br ₂ Cu ₂ P ₄
Formula weight	734.09	1179.76
Temperature [K]	120(2)	120(2)
Wavelength [Å]	0.71073	0.71073
Crystal system	monoclinic	monoclinic
Space group	<i>P2₁/c</i>	<i>P2₁</i>
Unit cell dimensions	<i>a</i> = 13.5328(4) Å, <i>a</i> = 90° <i>b</i> = 14.4864(5) Å, <i>β</i> = 92.407(2)° <i>c</i> = 16.3381(4) Å, <i>γ</i> = 90°	<i>a</i> = 11.2105(3) Å, <i>a</i> = 90° <i>b</i> = 18.7290(6) Å, <i>β</i> = 97.6364(17)° <i>c</i> = 12.1317(2) Å, <i>γ</i> = 90°
Volume [Å ³]	3200.12(17)	2524.60 (11)
<i>Z</i>	4	2
Density (calculated) [Mg m ⁻³]	1.524	1.552
Absorpt. coefficient [mm ⁻¹]	2.189	2.592
<i>F</i> (000)	1488	1192
Crystal size [mm]	0.52 × 0.45 × 0.10	0.10 × 0.10 × 0.08
<i>θ</i> range for data collection [°]	2.97 to 27.47°	3.39 to 27.48
Index ranges	-17 ≤ <i>h</i> ≤ 17 -18 ≤ <i>k</i> ≤ 18 -21 ≤ <i>l</i> ≤ 19	-14 ≤ <i>h</i> ≤ 14 -22 ≤ <i>k</i> ≤ 24 -15 ≤ <i>l</i> ≤ 15
Reflections collected	46486	30939
Independent reflections	7284 [<i>R</i> (int) = 0.0538]	10626 [<i>R</i> (int) = 0.0571]
Completeness to <i>θ</i>	99.4% (<i>θ</i> = 27.47°)	99.7% (<i>θ</i> = 27.48°)
Data / restraints / parameters	7284 / 0 / 380	10626 / 1 / 613
Max. and min. transmission	0.8108 and 0.3957	0.8195 and 0.7816
Refinement method	Full-matrix least-squares on <i>F</i> ²	Full-matrix least-squares on <i>F</i> ²
Goodness-of-fit on <i>F</i> ²	1.025	0.973
Final <i>R</i> indices [<i>I</i> > 2σ(<i>I</i>)]	<i>R</i> 1 = 0.0313, <i>wR</i> 2 = 0.0680	<i>R</i> 1 = 0.0374, <i>wR</i> 2 = 0.0613
<i>R</i> indices (all data)	<i>R</i> 1 = 0.0530, <i>wR</i> 2 = 0.0739 ^[a]	<i>R</i> 1 = 0.0569, <i>wR</i> 2 = 0.0666 ^[b]
Largest diff peak and hole [e Å ⁻³]	0.355 and -0.415	0.428 and -0.610

[a] $w = 1/[\sigma^2(F_o^2) + (0.0379P)^2 + 0.3987P]$, where $P = (F_o^2 + 2F_c^2)/3$. [b] $w = 1/[\sigma^2(F_o^2) + (0.0184P)^2]$, where $P = (F_o^2 + 2F_c^2)/3$.

UV/Vis (CHCl₃): λ_{max} (log ε) = 248 nm (4.09), 284 (4.31), 358 (3.94).

Synthesis of Complexes 3 and 4: 1,2-Bis(diphenylphosphanyl)benzene (446.5 mg, 1 mmol) was added to a suspension of copper(I) bromide or iodide (1 mmol) in 50 mL of dry acetonitrile, and the mixture was heated under reflux for 4 h. Slow evaporation of the resulting light-green solution at room temperature gave a crystalline solid, which was filtered off and dried in vacuo.

[Cu(μ₂-Br)(dppbz)]₂ (3): Light-green powder (550 mg, 93%), m.p. 295 °C. C₃₀H₂₄BrCuP₂ (589.93): calcd. C 61.08, H 4.10; found C 60.86, H 3.97. IR: ν̄ = 3415m, 3049w, 1637w, 1585m, 1480m, 1435s, 1184m, 1096m, 1027m, 750m, 744s, 695s, 518s, 497m, 482m cm⁻¹. UV/Vis (CHCl₃): λ_{max} (log ε) = 258 nm (3.71), 293 (3.68), 351 (3.63).

[Cu(dppbz)]_x (4): Light-green powder (541 mg, 85%), m.p. 298 °C. C₃₀H₂₄CuIP₂ (636.94): calcd. C 61.08, H 4.10; found C 56.15, H 3.89. IR: ν̄ = 3437m, 3048w, 1637m, 1585w, 1480m, 1434s, 1184w, 1156w, 1094m, 1027w, 759m, 741s, 691vs, 518vs, 496m, 480m cm⁻¹. UV/Vis (CHCl₃): λ_{max} (log ε) = 248 nm (4.35), 293 (4.16), 328 (4.07).

Synthesis of [CuI(dppbz)(2,4-dtucH₂)] (5): 1,2-Bis(diphenylphosphanyl)benzene (112 mg, 0.25 mmol) was added in small portions to a suspension of **4** (83 mg, 0.25 mmol) in 60 mL of dry acetone and the mixture was stirred for 1 h at 50 °C. The resulting clear solution was filtered and left to evaporate at ambient. The microcrystalline solid that was deposited upon standing for several days was filtered off and dried in vacuo. Orange powder (105 mg, 53%), m.p. 305 °C. C₃₄H₂₈CuIN₂P₂S₂ (781.16): calcd. C 52.28, H 3.61, N 3.59; found C 52.47, H 3.59, N 3.46. IR: ν̄ = 3216w, 3048m, 1610m, 1531s, 1480s, 1435s, 1185m, 1112m, 1095vs, 759m, 742vs,

692vs, 518vs, 496s, 480m cm⁻¹. UV/Vis (CHCl₃): λ_{max} (log ε) = 248 (4.36), 330 (4.04).

Synthesis of Complexes 6 and 7: A solution of 2,4-dithiouracil (144 mg, 1 mmol) in a small amount (≈20 mL) of methanol was added to a suspension of CuI or CuBr (0.5 mmol) in 30 mL of dry acetonitrile and the mixture was stirred for 2 h. The orange-yellow precipitate that deposited upon cooling was filtered off, washed with small amounts of THF and dried in vacuo.

[CuI(2,4-dtucH₂)]_x (6): Orange-red powder (155 mg, 93%), m.p. 295 °C. C₄H₄CuIN₂S₂ (334.68): calcd. C 14.36, H 1.20, N 8.37; found C 14.23, H 1.12, N 7.85. IR: ν̄ = 3212m, 3096w, 2975w, 1609vs, 1528vs, 1466m, 1260s, 1220s, 1195s, 1110vs, 983m, 856m, 789m, 692m, 671m, 462m, 395w cm⁻¹. UV/Vis (DMF): λ_{max} (log ε) = 284 (4.07), 352 (3.75), 397 (3.04).

[CuBr(2,4-dtucH₂)]_x (7): Orange-red powder (120 mg, 84%), m.p. 280 °C. C₄H₄BrCuN₂S₂ (287.67): calcd. C 16.70, H 1.40, N 9.74; found C 17.62, H 1.49, N 9.50. IR: ν̄ = 3198w, 3070m, 2985m, 2883m, 1616s, 1575s, 1551vs, 1481m, 1220m, 1125s, 744w, 693m, 518w cm⁻¹. UV/Vis (DMF): λ_{max} (log ε) = 284 (4.18), 354 (3.88), 403 (3.45).

Acknowledgments

We thank the EPSRC X-ray crystallography service at the University of Southampton for collecting the X-ray data.

[1] K. D. Karlin, J. Zubieta, *Copper Coordination Chemistry: Biochemical and Inorganic Perspectives*, Adenine Press, New York, 1983, and references cited therein.

- [2] B. Krebs, G. Henkel, *Angew. Chem. Int. Ed. Engl.* **1991**, *30*, 769–788.
- [3] P. Karagiannidis, P. Aslanidis, D. P. Kessissoglou, B. Krebs, M. Dartmann, *Inorg. Chim. Acta* **1989**, *156*, 47–56.
- [4] a) S. K. Hadjikakou, P. Aslanidis, P. Karagiannidis, A. Aubry, S. Skoulika, *Inorg. Chim. Acta* **1992**, *193*, 129–135; b) S. K. Hadjikakou, P. Aslanidis, P. Karagiannidis, D. Mentzafos, A. Terzis, *Inorg. Chim. Acta* **1991**, *186*, 199–204.
- [5] a) S. K. Hadjikakou, P. Aslanidis, P. Karagiannidis, D. Mentzafos, A. Terzis, *Polyhedron* **1991**, *10*, 935–940; b) S. K. Hadjikakou, P. Aslanidis, P. Karagiannidis, A. Hountas, A. Terzis, *Inorg. Chim. Acta* **1991**, *184*, 161–166.
- [6] P. J. Cox, P. Aslanidis, P. Karagiannidis, *Polyhedron* **2000**, *19*, 1615–1620.
- [7] a) P. Aslanidis, P. J. Cox, S. Divanidis, A. C. Tsipis, *Inorg. Chem.* **2002**, *41*, 6875–6886; b) P. Aslanidis, P. J. Cox, S. Divanidis, P. Karagiannidis, *Inorg. Chim. Acta* **2004**, *357*, 1063–1076.
- [8] a) M. Sigl, A. Schier, H. Schmidbaur, *Eur. J. Inorg. Chem.* **1998**, 203–210; b) L.-C. Song, J.-T. Liu, Q.-M. Hu, L.-H. Wenig, *Organometallics* **2000**, *19*, 1643–1647; c) W.-M. Xue, M. C.-W. Chan, Z.-M. Su, K.-K. Cheung, S.-T. Liu, C.-M. Che, *Organometallics* **1998**, *17*, 1622–1624; d) W.-M. Xue, Y. Wang, T. C. W. Mak, C.-M. Che, *J. Chem. Soc., Dalton Trans.* **1996**, 2827–2834; e) J. E. Barclay, A. Hills, T. C. W. Mak, D. L. Hughes, G. J. Leigh, *J. Chem. Soc., Dalton Trans.* **1988**, 2871–2877; f) D. Esjornson, M. Bakir, P. E. Fanwick, K. S. Jones, R. A. Walton, *Inorg. Chem.* **1990**, *29*, 2055–2061; g) J. M. Bevilacqua, J. A. Zuleta, R. Eisenberg, *Inorg. Chem.* **1994**, *33*, 258–266; h) K. D. John, K. V. Salazar, B. L. Scott, R. T. Baker, A. P. Sattelberger, *Organometallics* **2001**, *20*, 296–304; i) A. J. Paviglianiti, D. J. Min, W. C. Fultz, J. L. Burmeister, *Inorg. Chim. Acta* **1989**, *159*, 65–82; j) K. D. John, K. V. Salazar, B. L. Scott, R. T. Baker, A. P. Sattelberger, *J. Chem. Soc., Chem. Commun.* **2000**, 581–582.
- [9] W. Saenger, *Principles of Nucleic Acid Structures*, Springer, New York, Berlin, Heidelberg, Tokyo, **1984**, chapter 7.
- [10] a) Al M. Lamsabhi, M. Alcamí, O. Mó, M. Yáñez, *ChemPhysChem.* **2003**, *4*, 1011–1016; b) Al M. Lamsabhi, M. Alcamí, O. Mó, M. Yáñez, *ChemPhysChem.* **2004**, *5*, 1871–1878.
- [11] E. Shefter, H. G. Mautner, *J. Am. Chem. Soc.* **1967**, *89*, 1249–1253.
- [12] S. J. Bernes-Price, L. A. Colquhoun, P. C. Healy, K. A. Byriel, J. V. Hanna, *J. Chem. Soc., Dalton Trans.* **1992**, 3357–3363.
- [13] A. Cingolani, C. Di Nicola, Effendy, C. Pettinari, B. W. Skelton, N. Somers, A. H. White, *Inorg. Chim. Acta* **2005**, *358*, 748–762.
- [14] G. L. Soloveichik, O. Eisenstein, J. T. Poulton, W. E. Streib, J. C. Huffman, K. G. Caulton, *Inorg. Chem.* **1992**, *31*, 3306–3312.
- [15] A. Carvajal, X.-Y. Liu, P. Alemany, J. J. Novoa, S. Alvarez, *Int. J. Quantum Chem.* **2002**, *86*, 100–105.
- [16] P. Alemany, S. Alvarez, *Inorg. Chem.* **1992**, *31*, 4266–4275.
- [17] P. Karagiannidis, P. Aslanidis, S. Papastefanou, D. Mentzafos, A. Hountas, A. Terzis, *Polyhedron* **1990**, *9*, 981–986.
- [18] a) A. D. Becke, *J. Chem. Phys.* **1992**, *96*, 2155–2160; b) A. D. Becke, *J. Chem. Phys.* **1993**, *98*, 5648–5652.
- [19] C. Lee, W. Yang, R. G. Parr, *Phys. Rev. B* **1988**, *37*, 785–789.
- [20] a) N. Godbout, D. R. Salahub, J. Andzelm, E. Wimmer, *Can. J. Chem.* **1992**, *70*, 560–571; b) C. Sosa, J. Andzelm, B. C. Elkin, E. Wimmer, K. D. Dobbs, D. A. Dixon, *J. Phys. Chem.* **1992**, *96*, 6630–6636.
- [21] J. Andzelm, E. Wimmer, *J. Chem. Phys.* **1992**, *96*, 1280–1303.
- [22] S. K. Hadjikakou, C. D. Antoniadis, P. Aslanidis, P. J. Cox, A. C. Tsipis, *Eur. J. Inorg. Chem.* **2005**, 1442–1452.
- [23] H. B. Schlegel, *J. Comput. Chem.* **1982**, *3*, 214–218.
- [24] M. J. Frisch, G. W. Trucks, H. B. Schlegel, G. E. Scuseria, M. A. Robb, J. R. Cheeseman, V. G. Zakrzewski, J. A. Montgomery, T. Vreven, K. N. Kudin, J. C. Burant, J. M. Millan, S. S. Iyengar, J. Tomasi, V. Barone, B. Mennucci, M. Cossi, G. Scalmani, N. Rega, G. A. Petersson, H. Nakatsuji, M. Hada, M. Ehara, K. Toyota, F. R. J. Hasegawa, M. Ishida, T. Nakajima, Y. Honda, O. Kitao, H. Nakai, M. Klene, X. Li, J. E. Knox, H. P. Hratchian, J. B. Cross, C. Adamo, J. Jaramillo, R. Gomperts, R. E. Stratmann, O. Yazyev, A. J. Austin, R. Cammi, C. Pomelli, J. W. Ochterski, P. Y. Ayala, K. Morokuma, G. A. Voth, P. Salvador, J. J. Dannenberg, V. G. Zakrzewski, S. Dapprich, A. D. Daniels, M. C. Strain, O. Farkas, D. K. Malick, A. D. Rabuck, K. Raghavachari, J. B. Foresman, J. V. Ortiz, Q. Cui, A. G. Baboul, S. Clifford, J. Cioslowski, B. B. Stefanov, G. Liu, A. Liashenko, P. Piskorz, I. Komaromi, R. L. Martin, D. J. Fox, T. Keith, M. A. Al-Laham, C. Y. Peng, A. Nanayakkara, M. Challacombe, P. M. W. Gill, B. Johnson, W. Chen, M. W. Wong, C. Gonzalez, J. A. Pople, *Gaussian 03, Revision B.02*, Gaussian, Inc., Pittsburgh, PA, **2003**.
- [25] Z. Otwinowski, W. Minor, *Methods in Enzymology*, **1997**, volume 276: *Macromolecular Crystallography, Part A* (Eds.: C. W. Carter, Jr., R. M. Sweet), Academic Press, pp. 307–326.
- [26] R. Hoof, *COLLECT – Data collection software*, **1998**, Nonius B.V.
- [27] A. Altomare, M. C. Burla, M. Camalli, G. L. Casciarano, C. Giacovazzo, A. Guagliardi, A. G. G. Moliterni, G. Polidori, R. Spagna, *J. Appl. Crystallogr.* **1999**, *32*, 115–119.
- [28] G. M. Sheldrick, *SHELXL-97, A Program for crystal structure analysis (Release 97-2)*, University of Göttingen, Germany, **1997**.
- [29] L. J. Farrugia, *J. Appl. Crystallogr.* **1997**, *30*, 565.

Received: August 15, 2005

Published Online: December 5, 2005